International Journal of Engineering Research and Technology.
ISSN 0974-3154 Volume 4, Number 2 (2011), pp. 189-198

http://www.irphouse.com

# Influence of Strain Rate and Temperature on Superplastic Behavior of Sinter Forged Al6061/SiC Metal Matrix Composites

**A. Chennakesava Reddy**

*Professor, Department of Mechanical Engineering*
*JNTUH College of Engineering, Hyderabad – 500 085, Andhra Pradesh; India*
*E-mail: dr_acreddy@yahoo.com*

**Abstract**

Al6061/10%SiC metal matrix composites were prepared by cold pressing and sinter forging. The tensile tests were conducted on theAl6061/10%SiC composite specimens at high temperatures and different strain rates. The results conclude that the flow stress decreased with increasing temperature. The flow stress increased with increasing stain rate. The threshold stress increases as the temperature decreases. Al6061/10%SiC composite at $500^0$C exhibits superplasticity behavior.

**Keywords:** cold pressing, forging, flow stress, superplasticity.

## Introduction

Aluminum matrix composites reinforced with silicon carbide are attractive to industry because of high specific strength, high stiffness, high corrosion resistance, low density and thermal stability [1]. These composites have a desirable combination of room temperature specific strength and modulus and high temperature formability [2]. Grain refining of the materials has been attempted with significant success in developing superplastic composite materials [3]. It has been also reported that incipient melting at grain boundaries can contribute to high strain rate superplasticity. However, the superplastic deformation mechanisms in composites are still not well understood.

The objectives of this research are to manufacture aluminum matrix composites reinforced with silicon carbide by cold pressing and sinter forging methods and determine the optimum conditions for superplastic forging and evaluate the mechanical properties.

## Experimental Procedure

The Al6061-SiC composite was manufactured by mechanical alloying of mixed Al6061 and SiC powder and consolidated by cold pressing followed by sinter forging dry blend of the mechanical alloyed Al6061-SiC powder.

**Table 1:** Chemical composition of matrix alloy.

| Alloy | Composition determined spectrographically, % | | | | | | | | |
|---|---|---|---|---|---|---|---|---|---|
| | Al | Si | Fe | Cu | Ti | Mg | Mn | Zn | Cr |
| 6061 | 97.6 | 0.62 | 0.61 | 0.021 | 0.053 | 0.98 | 0.044 | 0.072 | 0.0051 |

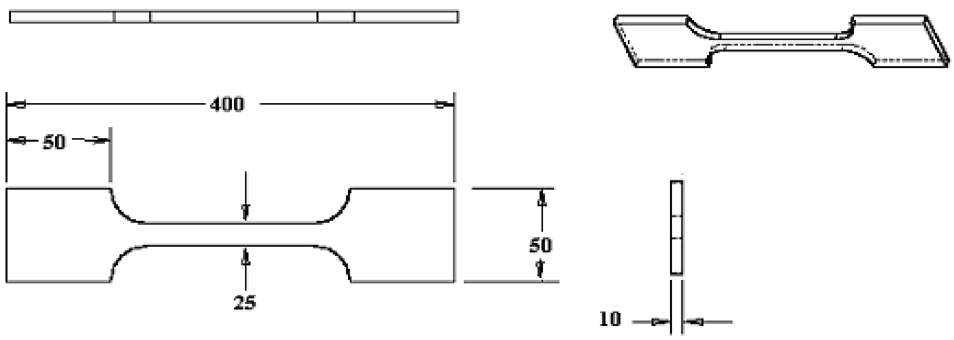


**Figure 1:** Tensile specimen, all dimensions are in mm.

The chemical composition of the Al 6061 powder is shown in Table 1. The average particle size of Al6061 is 60 μm. The average size of SiC particles is 5.0 μm. The Al6061 and SiC powders were mixed with composition having volume percent of 10% of SiC powder in a blender for 15 minutes. The composite manufacturing was carried out using cold pressing of the Al6061-SiC powder into a bar followed by sinter forging.

No binder was used to eliminate possible contamination, which could degrade the mechanical properties of the reinforcement and the matrix. Cold uniaxial pressing of the Al6061-SiC was performed at a pressure of 280 MPa in a rectangular steel die with 50x10 $mm^2$ cross sectional area using a die-wall lubricant in a 50-ton hydraulic press at room temperature. This was followed by sinter forging of the composites between compression platens coated with BN at a temperature of $500^0$C. A thermocouple inserted in the die was used to monitor the temperature and a pressure of 150 MPa for 15 minutes. After sinter forging was finished the sample was unloaded and the furnace cooled to room temperature. The samples were machined into a wedge type tensile bar for tension tests (figure 1).

The consolidated composites were characterized for mechanical properties and microstructure properties. The mechanical properties of these composites were characterized by tensile tests. The tensile specimens were machined parallel to the sinter forging direction by milling. The high temperature tensile tests were conducted at 400, 450, and 500$^0$C. The constant velocity tensile tests were carried out in air at room temperature, 400, 450, and 500$^0$C at a nominal strain rate of $10^{-2}$, $10^{-1}$ , and 1 $s^{-1}$ using an Instron servo controlled hydraulic universal testing machine in which the movement of the cross head is produced by a hydraulic cylinder. Molybdenum disulfide was used between the bolts and fixtures and caps as a lubricant for high temperature testing. The load displacement data were collected using Labview software for high-speed data acquisition and converted to the true tensile stress and strain assuming conservation of sample volume. The samples were heated in a muffle furnace to the testing temperature in about 1 hour and were held at testing temperature for 20 minutes before the test. The temperature was monitored and maintained constant within ±2$^0$C during the test. The tensile axis was selected to be parallel to the pressing plane.

The fracture surface microstructures of the compression and tensile test specimens were examined using optical microscopy and SEM. The microstructures were characterized by using optical microscopy and scanning electron microscopy. The fractured tensile specimens were examined using a JEOL scanning electron microscope (SEM).

## Results and Discussion

The optical micrograph of the composite surface perpendicular to the direction of sinter forging is shown in figure. It is free from cracks and close to full density, with no large pores. It is also clear that SiC segregates to the grain boundaries of the matrix.

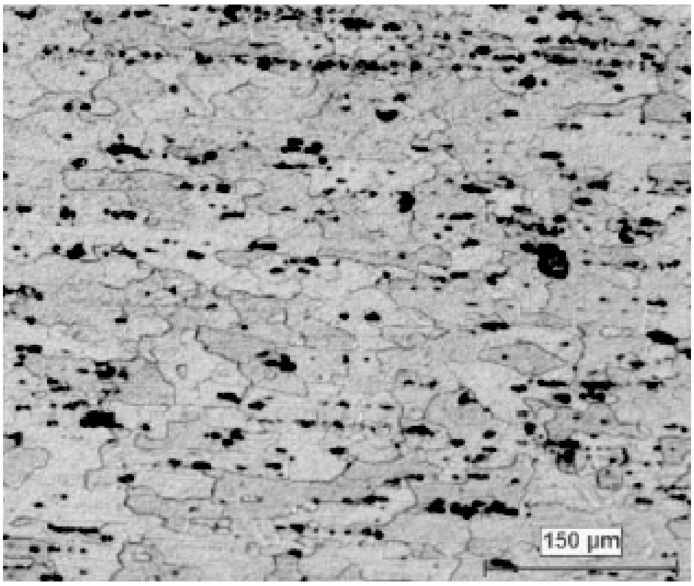


**Figure 2:** Optical micrograph of sinter forged Al6061/SiC composite at 500$^0$C.

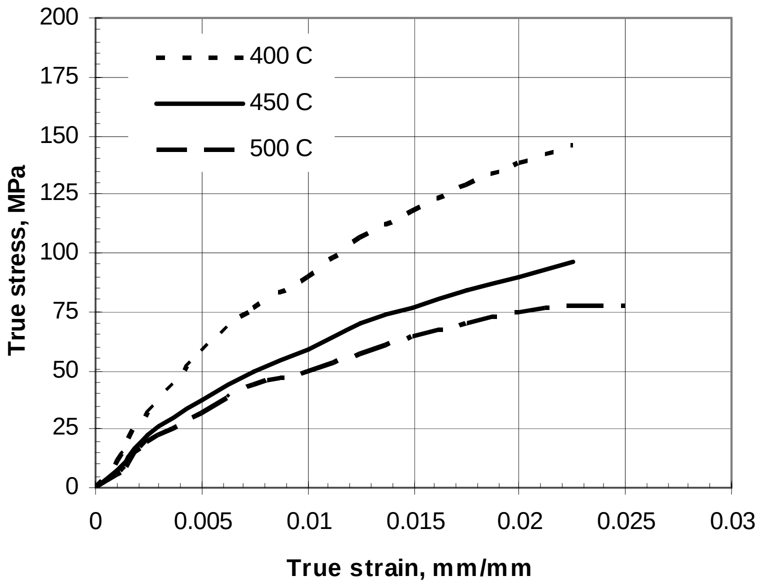


**Figure 3:** Effect of $10^{-2}$ $s^{-1}$ strain rate on true stress of Al6061/SiC composites.

True tensile stress-strain curves of Al6061/SiC composites at 400, 450 and $500^0$C as a function of strain rate are shown in figures 3, 4, and 5. In all cases, the flow stress decreased with increasing temperature. It is also observed that the flow stress increased with increasing stain rate (figure 6). The composites showed strain hardening behavior after yielding at all strain rates.

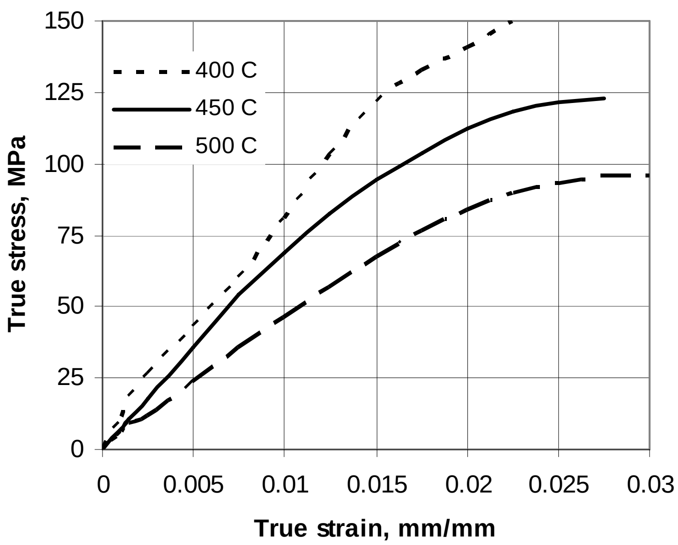


**Figure 4:** Effect of $10^{-1}$ $s^{-1}$ strain rate on true stress of Al6061/SiC composites.

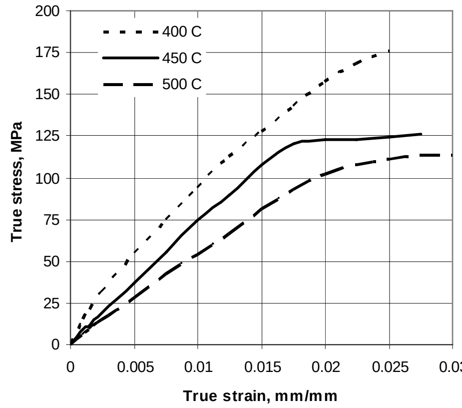


**Figure 5:** Effect of 1 $s^{-1}$ strain rate on true stress of Al6061/SiC composites.

At all temperatures the yield strength and ultimate tensile strengths increase as the strain rate increases (figure 7). The ultimate tensile strength is marginally higher than the yield strength. As the temperature increases, the yield and ultimate tensile strength decrease.

**Flow Stress-Strain Behaviour**

With increasing strain rate the flow stresses are increased at all temperatures. For the present study, the strain-rate sensitivity of the flow stress is represented by the empirical equation:

$$\sigma = K\dot{\varepsilon}^{m} \qquad (1)$$

where, *K* is a constant that signifies it is the material flow stress at a true strain rate of unity, $\dot{\varepsilon}$ is the true strain rate and *m* is the strain-rate sensitivity.

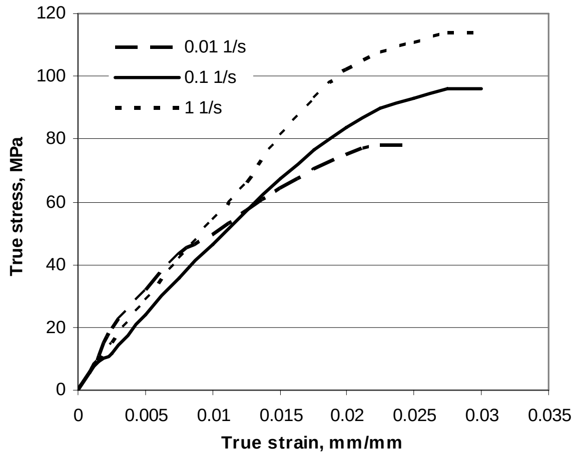


**Figure 6:** Effect of strain rate on true stress of Al6061/SiC composites.

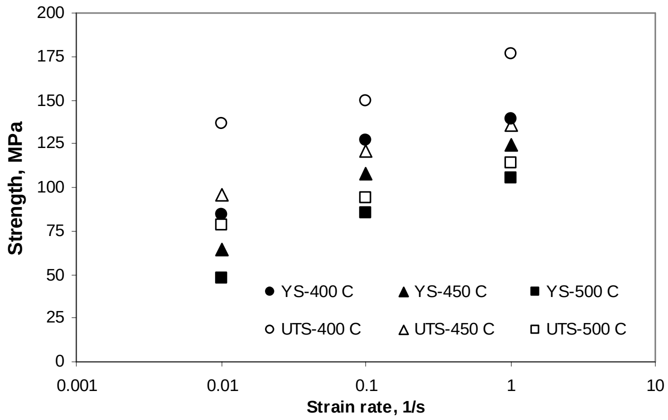


**Figure 7:** Effect of strain rate on yield and ultimate tensile strengths of Al6061/SiC composites.

The *m* value for the tension tests was determined from the flow stress at 2% true strain. The flow stress and the strain rate for each material was fitted to the standard power law relation and the *m* values are determined (figure 8). The standard power law relations are:

For temperature of $400^0$C

$$\sigma = 154.90\dot{\varepsilon}^{0.0275} \quad (2)$$

For temperature of $450^0$C

$$\sigma = 125.78\dot{\varepsilon}^{0.0678} \quad (3)$$

For temperature of $500^0$C

$$\sigma = 100.64\dot{\varepsilon}^{0.0668} \quad (4)$$

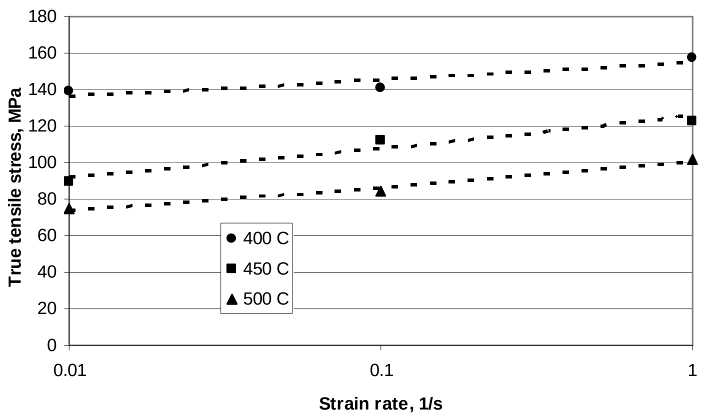


**Figure 8:** Determination of *m*, strain-rate sensitivity at 2% true strain.

The *m* values from the experiments are low compared with the values of *m* (> 0.3) expected for the observation of superplastic deformation. The low *m* value may be the result of a threshold stress ($\sigma_t$). This can be introduced into equation (1):

$$\sigma - \sigma_t = K_1 \dot{\varepsilon}^m \tag{5}$$

For slip accommodated grain boundary sliding, a strain rate sensitivity, *m*, of 0.5 is expected, which means that the stress exponent, *n* (=1/*m*), should be equal to 2. At *n* larger than 2, the threshold stress, is commonly invoked to account for higher apparent stress exponents. To determine the threshold stress, the researchers suggested a plot of $\dot{\varepsilon}^{1/n}$ (n = 2, 3, 4, 5) against $\sigma$ on a double linear scale and threshold stress is estimated by extrapolation to zero strain rate in the plot [5]. It was found in this study that $n = 3$ gave the best linear fit to the data. The plot of $\dot{\varepsilon}^{1/n}$ versus flow stress of Al6061/SiC composites are shown in figure 9 and the threshold stresses are shown in figure 10. The threshold stress increases as the temperature decreases.

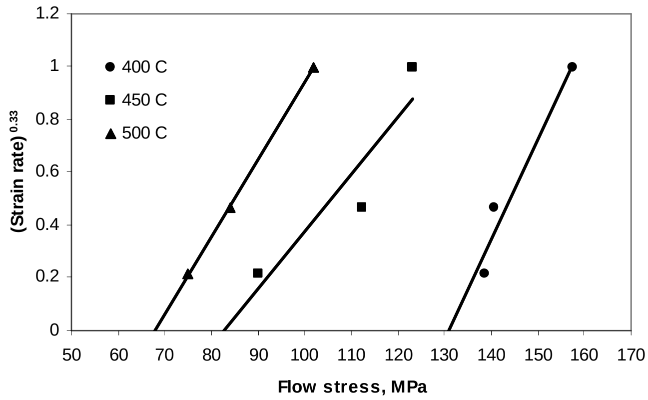


**Figure 9:** Determination of threshold stress at 2% true strain.

Taking the threshold stress into account, *m* value was determined from figure 10. The standard power law relations are:

For temperature of 400$^0$C

$$\sigma - \sigma_t = 23.207 \dot{\varepsilon}^{0.267} \tag{6}$$

For temperature of 450$^0$C

$$\sigma - \sigma_t = 34.416 \dot{\varepsilon}^{0.343} \tag{7}$$

For temperature of 500$^0$C

$$\sigma - \sigma_t = 48.28 \dot{\varepsilon}^{0.355} \tag{8}$$

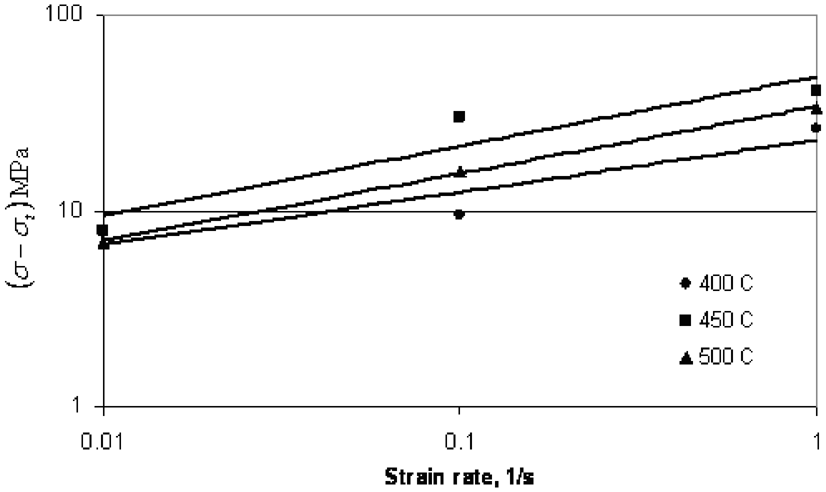


**Figure 10:** Determination of *m* values considering threshold stress at different temperatures.

The values of *m* (> 0.3) confirms of superplastic deformation at temperatures of 450 and 500$^0$C. Such a high *m* value is associated with an anomalous region in which diffusion accommodated flow and dislocation creep dominated flow are both operating. High values of *m* indicate resistance to neck development in tension. For the *m* values presented in this paper, the fracture of tensile specimens is shown in figure 11.

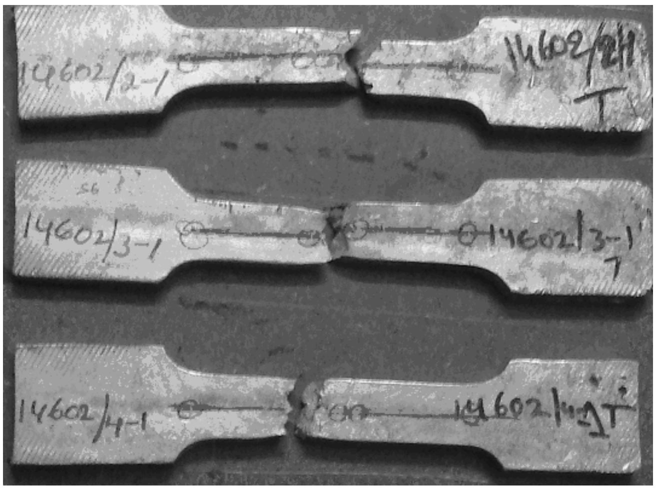

**Figure 11:** The fractured tensile specimens.

**Superplastic Mechanism**

During grain boundary sliding of a particle containing composite, the stress concentration at the particle-matrix interface has to be relaxed otherwise cavitation will occur. Mishra et al [6] constructed the mechanism map for aluminium matrix composite, according to this map if the interfacial sliding rates are lower than grain boundary sliding rate, this would lead to an inhomogeneous deformation and cavitation will increase which in turn prevents superplasticity. The map shows the change in mechanism is a function of reinforcement size, grain size and temperature. According to the superplastic mechanism map, it suggested a very high temperature deformation is required for high strain rate superplasticity, which is connected to the accommodation rate. According superplastic mechanism map (figure 12) Al6061/SiC composite at $500^0$C exhibits superplasticity.

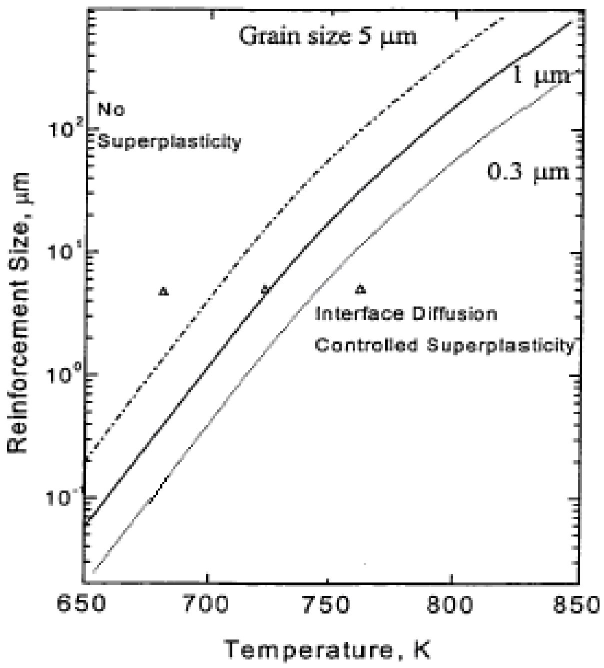


**Figure 12:** Superplastic mechanism map.

## Conclusions

The flow stress decreased with increasing temperature. The flow stress increased with increasing stain rate. The strain-rate sensitivity (m) values from the experiments are low compared with the values of *m* (> 0.3) expected for the observation of superplastic deformation. The low *m* value may be the result of a threshold stress ($\sigma_t$). The threshold stress increases as the temperature decreases. Al6061/SiC composite at $500^0$C exhibits superplasticity.

## Acknowledgements

The author acknowledges with thanks All India Council for Technical Education (AICTE) – New Delhi for sectioning R&D project, and Tapasya Casting Private

Limited – Hyderabad, and Indian Institute of Chemical Technology – Hyderabad for their technical help.

## References

[1] Mishra, R.S., and Mukherjee, A.K., 1991, "On Superplasticity in Silicon Carbide Reinforced Aluminium Composites," Scripta Metall. et Mater., 25, pp. pp.271-275.

[2] Nieh, T.G., and Chellman, D., 1984, "Modulus measurements in discontinuous reinforced aluminium composites," Scripta Metall., 18, pp.925-928.

[3] Biler, T.R., Mishra, R.S., and Mukherjee, A.K., 1996, "High strain rate superplasticity in aluminium-matrix composites," J. of Metals, pp.52-57.

[4] Chennakesava Reddy, A., 2004, "Experimental Evaluation of Elastic Lattice Strains in the Discontinuously SiC Reinforced Al-alloy Composites," Proc. National Conference on Emerging Trends in Mechanical Engineering, Nagapur, 05-06th February, Paper No. e-TIME/110/E-07, pp.81,.

[5] Mohmad, F.A., Park, K.T., and Lavernia, E.J., 1992, "Creep behavior of discontinuous SiC-Al composites," Mater. Sci. and Eng., A150, pp.21-35.

[6] Mishra, R.S., Bieler, T.R., and Mukherjeee, A.K., 1997, "Mechanism of high strain rate superplasticity aluminium alloys composites," Acta Metall. Mater., 45(2), pp.561-568.